Comparative Study of Insulin Chain-B in Isolated and Monomeric Environments under External Stress

Akin Budi,[†] F. Sue Legge,[†] Herbert Treutlein,[‡] and Irene Yarovsky*,[†]

Applied Physics, School of Applied Sciences, RMIT University, GPO Box 2476V, Melbourne, Victoria, 3001, Australia, and Cytopia Research Pty. Ltd., PO Box 6492, St. Kilda Road Central, Melbourne, Victoria, 8008, Australia

Received: January 14, 2008; Revised Manuscript Received: March 16, 2008

We have conducted a series of theoretical simulations of insulin chain-B under different electric field conditions. This work extends our previous studies of the isolated chain-B by including chain-A and revealing the effects of chemical stress. For this complete protein, we observed increased stability under ambient conditions and under the application of thermal stress, compared to isolated chain-B. On the other hand, the presence of chain-A enhanced the effects of the applied electric field. Under the static field, the presence of chain-A lowered the strength of the field necessary to stretch the protein. Under the oscillating fields, there was relatively less stretching due to the competitive alignment process of the three helical regions with respect to the field. At high field strengths, we observed that the high frequency oscillating field caused less secondary structure disruption than a lower frequency field of the same strength.

1. Introduction

While there have been a considerable number of studies performed to investigate the effects of the electromagnetic radiation on human tissues, none of these studies to date have yielded conclusive answers. Some studies indicated the presence of a "nonthermal" effect, which damages tissues without apparent change in temperature.[1,2] This effect is conjectured to be the result of a very rapid temperature change which occurs at a time scale faster than can be detected by conventional thermometry.[3] However, such a rapid increase of temperature may cause structural changes, which can alter protein conformation and, ultimately, its function. In addition, changes in protein conformation can lead to the formation of amyloid fibrils, which form the basis for "conformational" diseases such as Alzheimer's, cystic fibrosis, and variant Creutzfeldt−Jakob disease. We have previously studied the effects of such "instantaneous" temperature increases as well as of the electric field on isolated insulin chain-B.[4–7]

Insulin is a small hormone responsible for regulating blood sugar level and also functions as a weak growth hormone. The insulin monomer consists of two chains, A and B. Chain-A is 21 amino acid residues long with a structure consisting of two helices spanning residues A1−A8 and A13−A20, which are linked by a loop region and stabilized by an intrachain disulfide bond between residues A6 and A11. Chain-B is 30 residues long and consists of a variable N-terminal region, a central helix at B9−B19, a loop at B20−B23, and an extended C-terminus. The central helix B9−B19 is conserved between species and is flanked by two disulfide bonds connecting residues A7 and B7 and residues A20 and B19. These two disulfide bonds lock the two chains together and exert a stabilizing influence on the central helix of chain-B. Under normal physiological conditions, insulin forms dimers stabilized by hydrogen bonds between residues B24 and B26 of individual monomers.[8,9] These hydrogen bonds link the C-termini of the two monomers and form an antiparallel β-sheet structure. In the presence of ions such as Zn^{2+} and Cl^{-}, the insulin dimers can form tetramers and hexamers, with the ions acting as their crystal center.[10–12] The hexameric form is particularly important, as it is the form adopted when insulin is stored in the pancreas.[13]

The active form of insulin is believed to be a monomer, based on studies conducted on despentapeptide insulin (DPI), which lacks the ability to form dimers but retains the full hormone activity.[14] However, efforts to isolate the insulin monomer have so far been unsuccessful due to insulin's solubility and its propensity to aggregate.[15] There is also evidence that the observed conformation of the "native" insulin structure is an artifact of the crystallographic process, where contacts caused by the crystal packing of the molecules produce a structure different from the active form.[16,17] Most information on the native structure of monomeric insulin has been obtained from nuclear magnetic resonance (NMR) studies of engineered monomeric insulin, DPI, with the active conformation identified to be analogous to the T-state.[18,19] Experimental studies on physiologically active monomeric forms of insulin have observed fluctuations in the N-terminus of chain-B[15,18,20,21] as well as flexible regions in the C-terminus of the chain.[18,21–23] The importance of such flexibility has also been demonstrated by the loss of activity shown by insulin when residues A1 and B29 are cross-linked.[24,25] This indicates that the native insulin monomer is intrinsically flexible and this property is essential to the interaction of insulin with its receptor.[16,18]

Chain-B has been shown to be stable independently of chain-A[26,27] and has been implicated in receptor binding mechanisms. There are many tertiary structural variations in chain-B, mostly occurring in the N-terminal region.[10,11,28–30] The two main conformational states are the R- and T-states.[31] In the R-state, residues B1−B8 are in an α-helical conformation, so that the overall helical region extends from B1 to B19. In the T-state, residues B1−B8 are in an extended conformation. In addition to the R- and T-states, other conformations have

* Corresponding author. Phone: +61 3 9925 2571. Fax: +61 3 9925 5290. E-mail: irene.yarovsky@rmit.edu.au.
[†] RMIT University.
[‡] Cytopia Research Pty. Ltd.

10.1021/jp800350v CCC: $40.75
Published on Web 06/07/2008

been observed, such as the R^f-state ("frayed"-state)[12,29] and the O-state.[30] In the R^f-state, residues B1−B3 are in an extended conformation, while residues B4−B8 are in an α-helical conformation. The O-state ("open"-state) is almost identical to the T-state, the difference being the extended B1−B8 residues are further away from the main body of the insulin molecule, and are thought to be involved in receptor binding.

In our previous molecular dynamics (MD) studies, we confirmed the flexibility of the isolated insulin chain-B and observed the formation of the T-like state.[4,5] By comparing the simulation results with NMR data on insulin chain-B in solution, we demonstrated that our simulation adequately sampled experimentally observed insulin conformations.[4] In subsequent studies, we have analyzed the response of insulin chain-B to thermal and electric field stress.[6,7] The studies revealed the difference in the structural and dynamical changes inflicted by the application of static and oscillating electric fields on insulin chain-B. Whereas the application of static fields restricted the flexibility and interfered with the normal dynamic behavior of the peptide, the application of oscillating fields caused the rapid alignment of the peptide along the electric field direction and subsequent loss of the secondary structure. Different oscillating field frequencies were also explored in the study, which showed that the frequency dependent effect only came into play at high field strengths.[7] The dipole moment of the peptide was observed to interact more closely with the applied field of frequency 1.225 GHz compared to the field of frequency 4.9 GHz.

This paper expands our previous studies by incorporating chain-A of insulin into the simulations. The complete insulin monomer is subjected to thermal stress and static and oscillating electric fields of several frequencies. The results of these simulations are compared to the data obtained under ambient conditions and those of the corresponding isolated chain-B systems. For consistency with the previous studies, the main frequency used for the oscillating field was 2.45 GHz, with selected systems simulated at frequencies of 1.225 and 4.9 GHz to enable observation of frequency dependent effects.

2. Methods

This study utilizes the classical molecular dynamics algorithm[32,33] as implemented in NAMD.[34] The well-validated, all-atom CHARMM27 force field[35] was chosen to represent the interactions between atoms. As in our previous studies,[4–7] the amino acids Glu, Arg, and Lys were charged according to the CHARMM27 force field, the His residues were protonated, and both termini regions and titratable side chains were charged, resulting in a neutral to acidic pH environment. The nonbonded potential function was multiplied by a linearly decaying switching function between 10 and 12 Å, which results in no interaction beyond 12 Å. Particle mesh Ewald summation was employed to account for long-range electrostatics.[36–38] A neighbor list was maintained for atoms within a 14 Å radius.

The lengths of covalent bonds involving hydrogen atoms have been fixed to their energy minimized values by utilizing the SHAKE algorithm.[39] This allowed us to ignore vibrational modes of hydrogen bonds and use a longer time step of 2 fs for all of the simulations. The starting coordinates for each system were taken from the Protein Data Bank.[40] We have chosen the wild boar insulin hormone (PDB accession code 1ZNI[10]) for this study. This particular insulin structure has an R^f form for its chain-B,[12,29] with residues B1−B3 and B24−B30 in the extended conformation, residues B4−B19 in the α-helical conformation, and residues B20−B23 forming a turn. The complete monomer of the insulin hormone, along with its disulfide bonds, is shown in Figure 1.

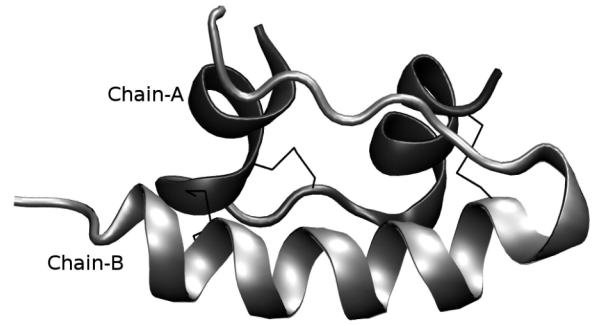

Figure 1. The starting insulin structure used in this work. Chain-A is shown in dark gray, chain-B is shown in light gray, and the disulfide bonds connecting them are shown as black lines.

TABLE 1: Summary of Systems Used in This Work (All of These Systems Simulated for 10 ns)

				oscillating systems		
temperature (K)	no electric field	electric field strength (V/m)	static systems	2.45 GHz	1.225 GHz	4.9 GHz
300		10^9	SM1	OM1		
		5×10^8	SM2	OM2	OM2H	OM2D
		10^8	SM3	OM3	OM3H	OM3D
		5×10^7	SM4	OM4		
		10^7	SM5	OM5	OM5H	OM5D
	NM300	0				
400	NM400	0				

The protein was enclosed in a periodic box sized 60 Å × 60 Å × 60 Å. After filling the box with 6879 TIP3P[41] water molecules (corresponding to a water density of 1.0 g/cm^3), the whole system was energy minimized for 20 000 steps by conjugate gradient and line search algorithms. For each simulated temperature, 300 and 400 K, two equilibration stages were then performed successively, each lasting 600 ps. The first of these stages was performed in a constant volume (NVT) ensemble. This was followed by constant pressure (NPT) equilibration at 1 bar, utilizing the Nosé−Hoover method of pressure control in which fluctuations in the barostat are controlled by Langevin dynamics,[42] as implemented in NAMD. The dynamics (data collection) stage was then performed in a constant pressure (NPT) ensemble set to 1 bar with thermal bath coupling to either 300 or 400 K for 10 ns. The atomic coordinates were saved every 2500 steps (5 ps) for analysis, resulting in 2000 trajectory frames for each run. The validity of this methodology has been tested in our previous study,[4,6] which reproduced the known behavior of insulin with the majority of the sampled conformations satisfying the nuclear overhauser effect (NOE) distance restraints obtained by NMR spectroscopy.[26]

The full list of simulated systems and details used in this work are given in Table 1. In the system nomenclature, we have used the letter "M" to denote monomeric insulin, "N" to denote no electric field, "S" to denote static field, and "O" to denote oscillating field.

3. Results and Discussion

3.1. Secondary Structure Evolution and Helical Content. The secondary structure evolution of insulin chain-B under monomeric conditions is obtained using the STRIDE algorithm,[43] and the plots are presented in Figure 2. In contrast to the secondary structures of the isolated chain-B,[6] the secondary

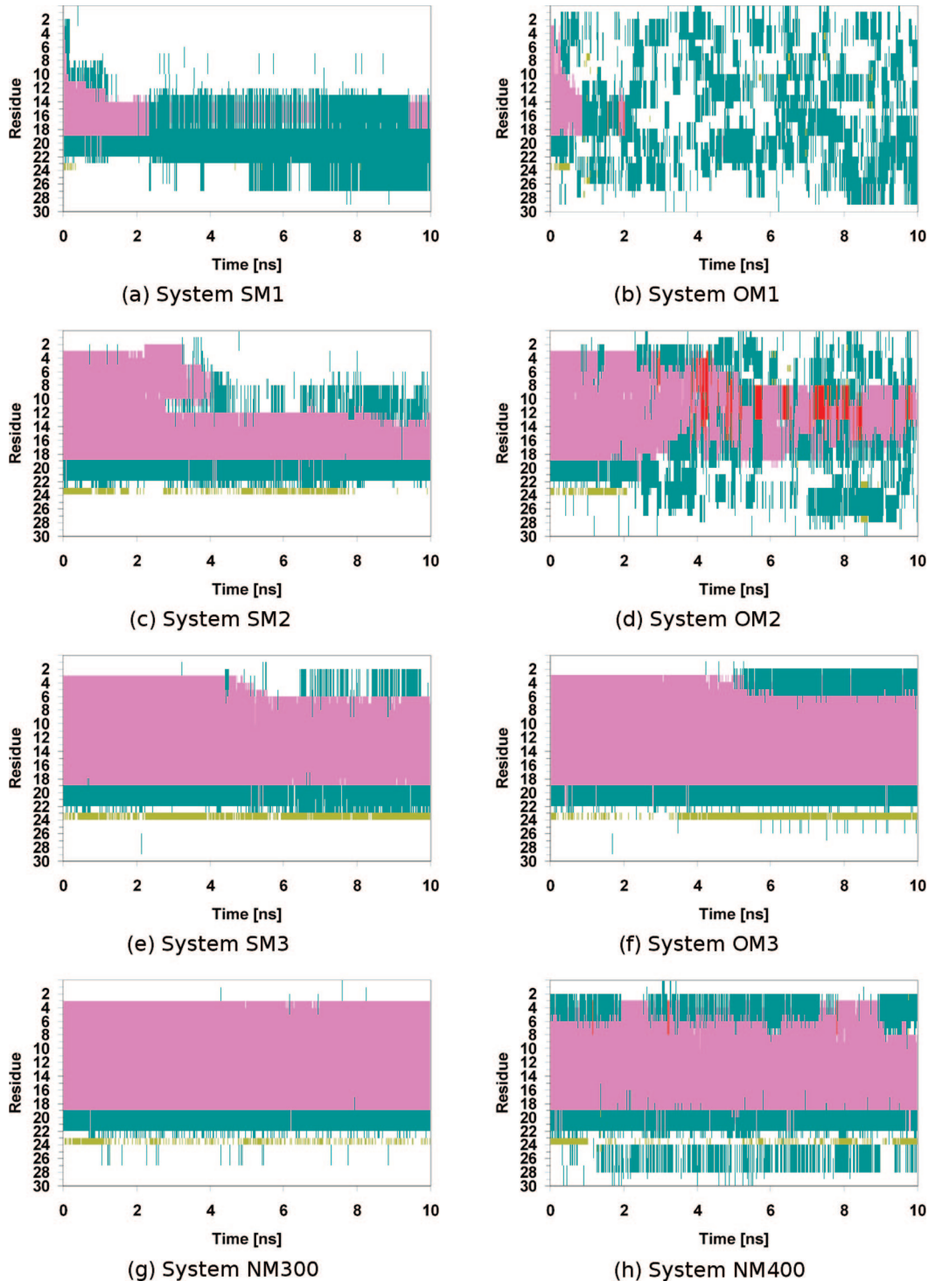

Figure 2. Secondary structure evolution of chain-B in selected monomeric insulin systems under static and oscillating electric field and thermal stress. The color codes denote the following secondary structure elements: magenta, α-helix; red, π-helix; cyan, turn; white, coil.

structure of the monomeric systems was observed to be very stable. This is not surprising, as the disulfide bonds between residues A7 and B7 and between residues A20 and B19 anchor the central helix of insulin chain-B, which results in remarkable stability even under the thermal stress and electric field stress of up to 10^8 V/m, apart from some minor fraying at the termini. The stability of these systems leads to the lack of α- to π-helix transition observed in our previous work.[4,6,7] In addition, no helix-breaking event at residue B8 was observed within the time scale of the simulations. It must be stressed that the helix breaking is integral for the normal activity of insulin which involves the transition from the R-state to the active T-state conformation. Some structural changes were observed in the thermally stressed system, and systems under static field of strengths 10^8 V/m and above. In the case of thermal stress, the changes were limited to the increased mobility of both termini, such as localized fraying around these regions. In systems SM1 and SM2, a helix-breaking event at the valine residue B12 was observed, which is similar to the one observed in isolated chain-B exposed to a static electric field of 10^9 V/m.[6] In system OM1, complete loss of the helical content was observed within 0.9 ns (2.2 electric field oscillations). This is slightly faster than

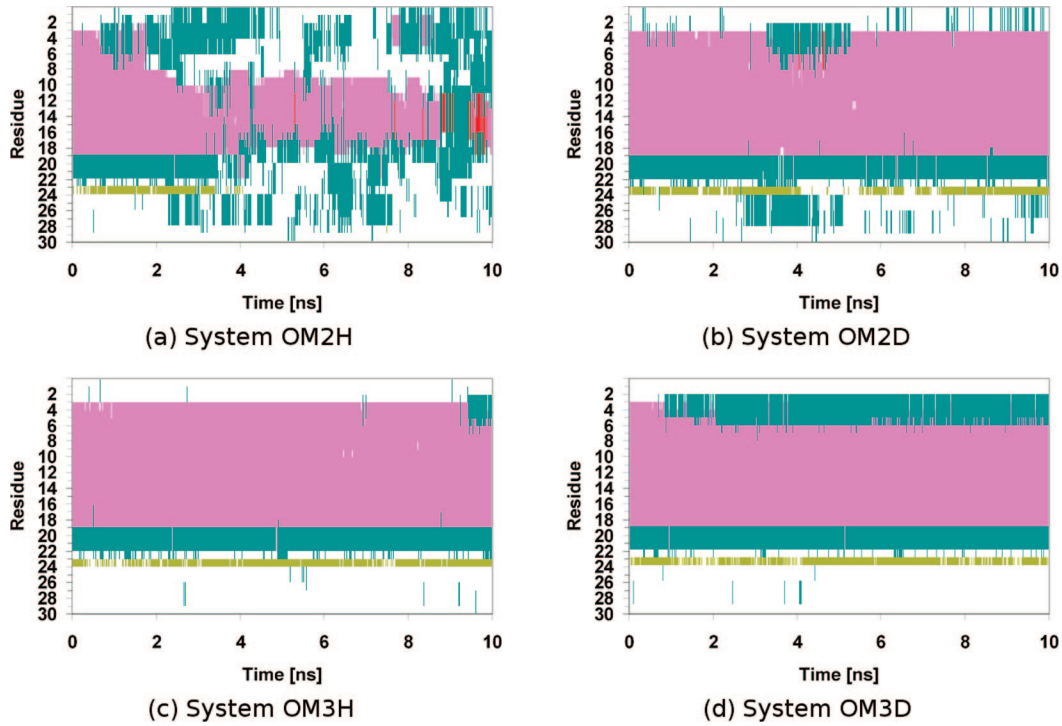

Figure 3. Secondary structure evolution of chain-B in selected monomeric insulin systems showing the frequency dependent effect. The color codes are the same as those for Figure 2.

the time it took to lose all helical content in the isolated chain-B system (1.2 ns).[6]

Figure 3 shows the frequency dependent effect observed in the oscillating field systems at a field strength of 5×10^8 V/m. System OM2D did not show any significant changes compared to systems OM2 and OM2H. This is because, at a frequency of 4.9 GHz, the oscillating field changes direction so rapidly that the protein is only exposed to a strong "instantaneous" field for a brief amount of time in each cycle. In system OM2H, insulin chain-B experienced more time under the influence of the field before it changed direction (refer to Budi et al.[7]), thus causing stretching of the helical region, similar to that experienced by system SM2. Insulin chain-B in a monomeric environment under oscillating electric field stress of strength 5×10^8 V/m was shown to generally experience less secondary structure damage compared to the isolated state. This is a direct result of the stability due to the presence of the disulfide bonds.

Figure 4 shows the percentage of retained helical content in residues B9−B19 of chain-B under electric field stress above 10^8 V/m. The figure shows that the secondary structure is dominated by α-helices. System SM1 exhibits a total loss of the helical content within 2 ns, and system SM2 exhibits a 40% loss within 2.5 ns. The disruptions experienced by these two systems are most likely caused by the presence of the two additional helices from the accompanying chain-A, which contributes to the enhancement of the dipole moment of the whole protein. This enhanced dipole moment allows the protein to interact more strongly with the applied static field, which caused the protein to align itself along the field direction and led to the stretching of the helical region. The loss of helical content due to the application of static field on chain-B of monomeric insulin occurred at a lower field strength (5×10^8 V/m) compared to the isolated case (10^9 V/m).[6]

In system OM1, the helical content was lost within 0.9 ns, which agrees with the visual observation of the secondary structure map in Figure 2. In system OM2, the helical content was reduced to an average of 50% after 2.5 ns, similarly to system OM2H. In contrast, system OM2D retained all of its B9−B19 helical content to the end of the simulation, albeit with some variations at around 4 and 8 ns. These variations indicate that some disruption to the secondary structure did occur throughout the simulation but was quickly repaired by the protein.

Table 2 presents the retained number of α-helical residues averaged over the whole data collection stage. Only the number of α-helical residues is presented, since no transition toward π-helix was observed. Similarly to the isolated chain-B systems,[6] chain-B in a monomeric environment under thermal stress was observed to lose approximately 16% of its α-helical content. The loss of the helical content in system NM400 occurs closer to the N-terminus as a consequence of the increased mobility around that region. Because of the disulfide bonds bracketing residues B7−B19, the helicity of residues B9−B19 is fully maintained in both the ambient and thermally stressed systems. Increased flexibility was also observed at the C-terminal region, as shown in the secondary structure plot (Figure 2).

Table 2 also confirms the loss of α-helical content of the systems at the two highest electric field strengths, with the exception of system OM2D. The variances of systems OM1, OM2, and OM2H were shown to be generally larger than the variances of the equivalent static field systems, which confirms the previous observation of the damage mechanism of the applied oscillating electric field, whereby an oscillating field causes the peptide to undergo continuous stretching and relaxation which causes it to unfold.[6] In system OM2D, most of the helical content is retained. This is likely because, at high frequency, the protein is only briefly exposed to high strength instantaneous electric field before the field changes direction.[7] Consequently, the oscillating field is only causing the alignment but not the stretching of the molecules. Interestingly, the number of helical residues lost due to increased temperature is comparable to the number lost at field strength over 10^8 V/m.

3.2. Dipole Moment Distribution. The monomeric insulin contains three helical regions—in addition to the helical part of

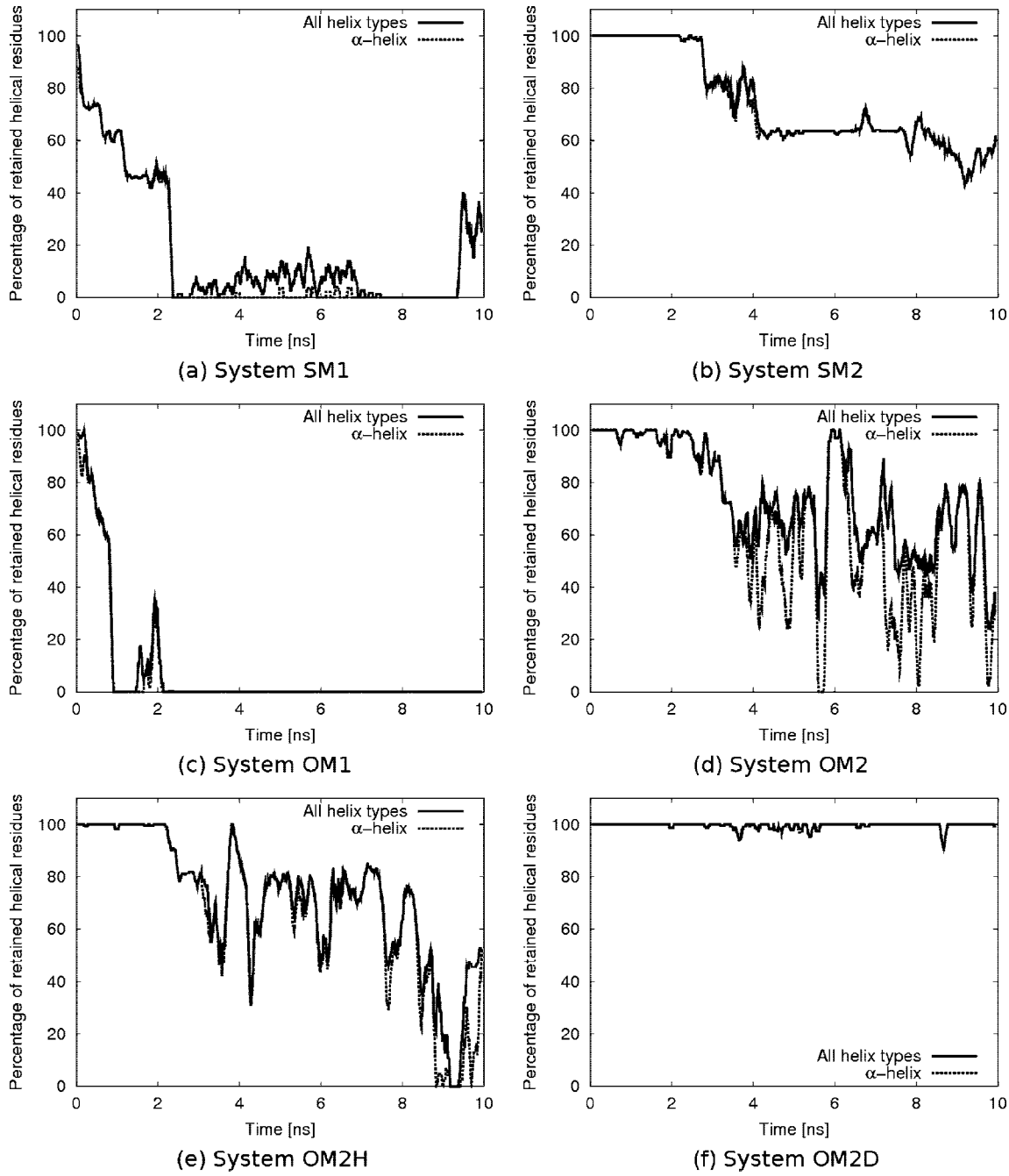

Figure 4. 100 ps running average of the retained B9−B19 helical content as a function of time for selected systems of monomeric insulin under electric field stress. The solid lines indicate the all-helical content, and the dotted lines indicate the α-helical content.

TABLE 2: Retained Number of α-Helical Residues for Chain-B in a Monomeric Environment under Electric Field Stress, Averaged over the Data Collection Stage, except Systems OM1 Where Averaging Was Performed over the First 2 ns

	retained α-helical residues			
system name	SM	OMH	OM	OMD
1	1.7 ± 2.9		4.2 ± 4.9	
2	10.0 ± 4.4	8.3 ± 4.3	9.0 ± 5.1	15.3 ± 1.4
3	14.4 ± 1.6	15.8 ± 0.7	14.6 ± 1.5	13.4 ± 1.0
4	15.3 ± 1.1		16.0 ± 0.1	
5	16.0 ± 0.3	13.8 ± 1.4	16.0 ± 0.2	15.0 ± 1.3
NM300	16.0 ± 0.2			
NM400	13.5 ± 1.6			

chain-B, helices A1−A8 and A13−A20 are also present. As the electric field is applied, the dipole moments of these three helices interact with each other and the electric field, and the helices align in the direction of the applied field. The resulting combined dipole moment of the entire molecule is larger than the dipole moment of each individual helix.

Distributions of the dipole moment in the *z*-direction for the B9−B19 region of the insulin chain-B in a monomeric environment under the electric field stress are plotted in Figure 5, along with the dipole moment distribution of the reference systems for comparison. The plots have been normalized to allow direct comparison. Overall, the plots are consistent with the previously observed results for the isolated chain-B systems.[6,7] The reference and the thermally stressed systems yield a uniform distribution centered around zero. Under static fields, the dipole

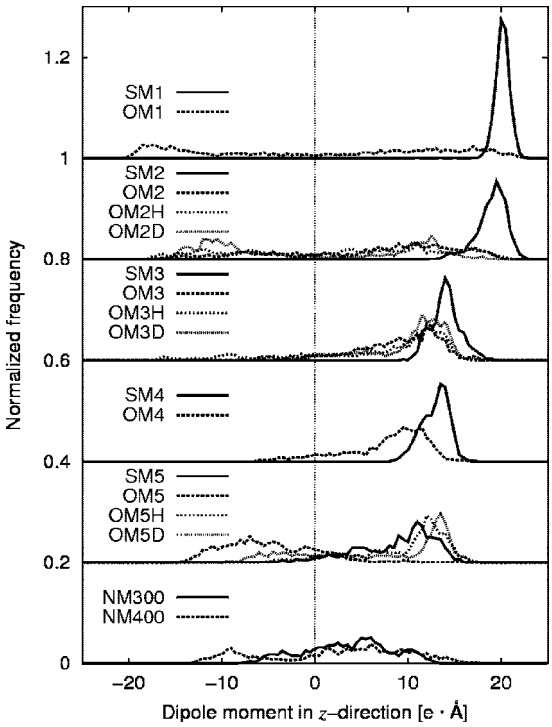

Figure 5. B9−B19 helical dipole moment distribution in the *z*-direction of insulin chain-B in the monomeric environment. Each plot has been displaced by 0.2 to improve clarity. Positive dipole moment signifies positive correlation with the electric field.

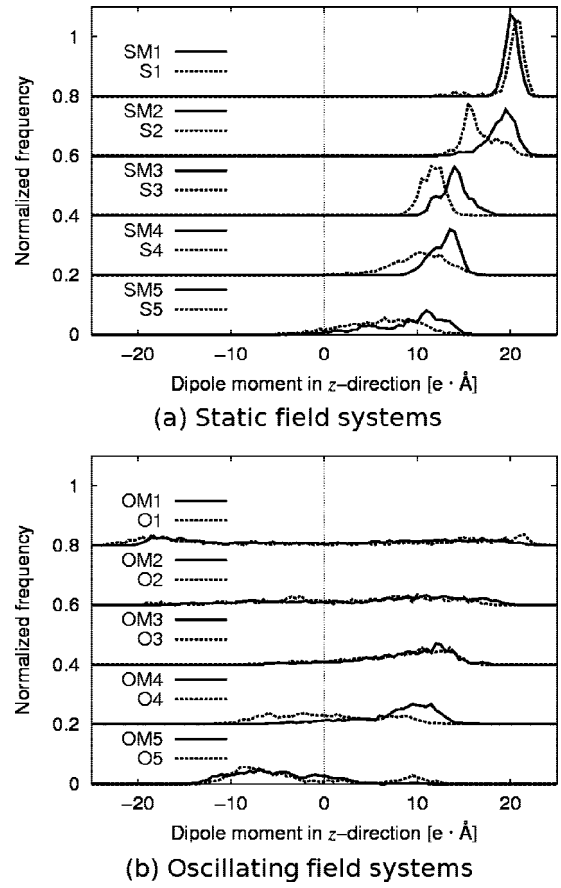

Figure 6. Comparison between the dipole moment in the *z*-direction between insulin chain-B in the isolated (dotted line)[6] and monomeric (solid line) environments.

moment distribution peaks at a positive value, indicating a situation where the B9−B19 helix axis is parallel to the direction of the applied field. In the case of the oscillating field, two typical situations were observed: a double peak, where the helix is continuously realigning with respect to the field direction, and a skewed distribution, where the molecule is not moving fast enough to align with the electric field. The skewed distribution is more prevalent at the lower electric field strength, as observed in Figure 5, because the electric field is not strong enough to cause near-instantaneous response of the protein as the field changes direction.

Figure 6 shows a comparison of the dipole moment distribution between insulin chain-B in isolated and monomeric environments at different electric field strengths. The data for the isolated chain-B have been reproduced from Budi et al.[6] for comparison. The figure shows that the distribution of the dipole moment for chain-B in a monomeric environment under static field stress is sharper and less spread compared to the isolated case, especially at the strongest field strength of 10^9 V/m. This is a consequence of the stronger overall dipole moment possessed by the monomeric insulin compared to isolated chain-B. In the higher field strength systems, all three helices of the monomeric insulin experience the effect of the electric field, resulting in a stronger coupling between the whole protein and the applied electric field. Because of the stronger coupling, insulin chain-B in a monomeric environment is able to align with respect to the field direction at a lower field strength than the isolated chain-B. Under the oscillating field, no coupling was observed, as is evident by the same absolute values of the dipole moment for each electric field strength of both systems.

The strong correlation between the helical dipole moment and the electric field is also evident from the time evolution of the dipole moment in the *z*-direction for the two lowest field strengths, shown in Figure 7. Chain-B in a monomeric environment consistently shows a higher value for the dipole moment, indicating stronger alignment with the electric field, compared to the isolated chain-B.

3.3. Root Mean Square Deviation (rmsd). The rmsd's of the B9−B19 helix backbone atoms under electric field stress were calculated relative to the start of the data collection stage. These are plotted in Figure 8 for all systems and averaged over 100 ps for clarity. The thermally stressed system and the systems at low field strengths were more stable with the average rmsd's never exceeding 0.7 Å. The static field systems were observed to reach their equilibrium values relatively quickly, after which the rmsd's showed little fluctuations. This behavior was shared by the systems under an oscillating field frequency of 1.225 and 2.45 GHz, although with more variation over time compared to the static field system. A notable exception is system OM2D which had a relatively stable rmsd of 0.66 Å. It is interesting that variations in the instantaneous rmsd values were observed, which indicate that the overall relative stability occurs because the whole protein is only briefly (almost instantaneously) exposed to the strong electric field before the field changes its direction, enabling the molecule to repair the conformational changes that might have occurred during the "instantaneous" exposure.

The average rmsd values for the last 1 ns of the simulations are presented in Table 3, together with the reference systems, NM300 and NM400. The only exception is system OM1, which had been averaged between 1 and 2 ns, where the helical secondary structure was still present. The rmsd's of the systems under an electric field strength of 10^8 V/m and below were found to be very stable with little deviations from the normal rmsd's of the reference system NM300. This indicates that the static

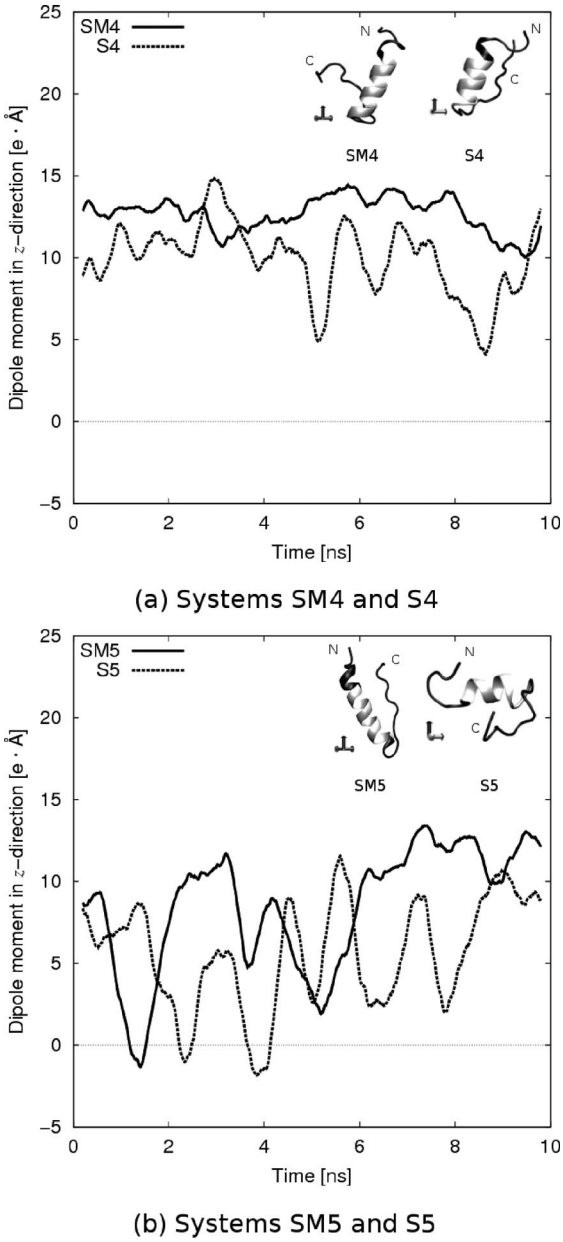

Figure 7. Time evolution of the dipole moment in the z-direction for selected systems. The data for the isolated chain-B have been reproduced from Budi et al.[6] The inset shows the conformation adopted by the peptide at the end of the simulation.

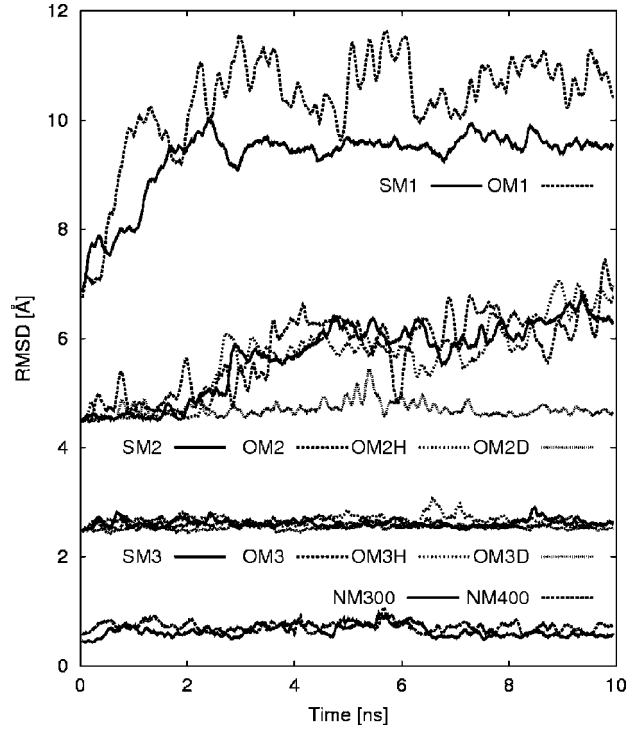

Figure 8. 100 ps running average of the B9−B19 helix backbone rmsd of selected monomeric insulin systems under the applied stresses. Each of the plots has been displaced by 2 Å for clarity.

TABLE 3: Average rmsd of Residues B9−B19 in Monomeric Insulin Systems (See Text for Details)

	rmsd (Å)			
system name	SM	OMH	OM	OMD
1	3.5 ± 0.1		3.7 ± 0.4	
2	2.5 ± 0.2	2.7 ± 0.2	2.6 ± 0.5	0.66 ± 0.09
3	0.62 ± 0.09	0.59 ± 0.07	0.62 ± 0.09	0.51 ± 0.05
4	0.65 ± 0.07		0.48 ± 0.08	
5	0.68 ± 0.08	0.53 ± 0.06	0.7 ± 0.1	0.59 ± 0.09
NM300	0.56 ± 0.09			
NM400	0.7 ± 0.1			

TABLE 4: Radius of Gyration of Chain-B in Each Monomeric Insulin System under Electric Field Stress, Averaged over the Data Collection Stage, after the First 1 ns

	r_g (Å)			
system name	SM	OMH	OM	OMD
1	19.4 ± 0.4		13.3 ± 2.4	
2	14.9 ± 0.3	12.1 ± 1.2	12.7 ± 1.5	11.0 ± 0.6
3	11.8 ± 0.7	10.9 ± 0.2	10.6 ± 0.3	10.6 ± 0.2
4	12.2 ± 0.5		11.0 ± 0.2	
5	10.9 ± 0.2	10.53 ± 0.25	11.05 ± 0.15	11.0 ± 0.2
NM300	11.2 ± 0.2			
NM400	10.55 ± 0.35			

electric fields of moderate strength have very little effect on the conformation of the helical region of insulin chain-B in a monomeric environment, similar to the thermal stress (NM400). A measurable effect was only observed at very high electric field strengths. It was previously shown that the oscillating electric field strength of 5×10^8 V/m was required to disrupt the secondary structure of isolated chain-B.[6,7] This trend is also observed in a monomeric environment, except for system OM2D. In general, the application of an electric field of strength 5×10^8 V/m disrupted the conformation of chain-B in a monomeric environment to a larger extent than it did to the isolated chain-B.[6] This is likely because of the presence of two helical regions of chain-A, which, as discussed previously, enhance the effect of the electric field due to the coupling of all helical dipole moments. In system OM2D, the whole protein only experiences brief periods of strong instantaneous electric field as the oscillating field nears its maximum amplitude, which are not enough to cause stretching of the B9−B19 residues. In the other oscillating field systems, more changes to the secondary structure were observed compared to the application of static fields of similar strengths.

3.4. Radius of Gyration (r_g). Table 4 shows the r_g values of the insulin chain-B in a monomeric environment, averaged over the data collection stage, after the first 1 ns. The r_g values are larger compared to the isolated chain-B systems.[6] This is due to the higher stability of the monomeric insulin where disulfide bonds between the two chains prevent chain-B to collapse into more compact conformations. System NM400 was

TABLE 5: Percentage of Solvent Accessible Surface Area of Chain-B under Monomeric Conditions

	percentage SASA (relative to NM300)			
system name	SM	OMH	OM	OMD
1	121.5 ± 1.3		109.8 ± 7.9	
2	110.4 ± 1.5	102.1 ± 5.2	101.8 ± 6.4	95.0 ± 5.7
3	98.9 ± 2.8	93.7 ± 2.9	91.6 ± 4.0	89.8 ± 2.9
4	100.9 ± 2.4		95.7 ± 2.0	
5	95.0 ± 1.9	89.0 ± 3.9	94.9 ± 1.9	94.6 ± 2.3
NM300	100.0 ± 1.8			
NM400	94.1 ± 4.4			

observed to have a smaller r_g value compared to system NM300. This is due to the increased kinetic energy, which allowed the protein to adopt a more compact conformation. The increase in flexibility is also evident in the higher variance exhibited in the NM400 system, compared to the NM300 system.

For the two highest electric field strengths simulated (5×10^8 and 10^9 V/m), the r_g value became very large, corresponding to the significant disruption to the secondary structure. The variance of these systems highlighted the different mechanism of damage caused by the oscillating electric field compared to the static electric field. Specifically, the application of static electric field on monomeric insulin caused stretching of the protein, which is accompanied by the restriction of the mobility and flexibility of the molecule. In contrast, the application of oscillating electric field, while causing the increase of mobility and flexibility of the protein, results in a more compact (collapsed) structure, as reflected by a lower r_g value and larger variance. Interestingly, system OM2D showed a similar r_g value to that of system NM300 (unstressed), albeit with a large variance. This is probably because, in system OM2D, the protein spends more time rotating to align itself with respect to the field direction than it is being stretched by the electric field. This is consistent with the observations of the secondary structure evolution (Figure 3) and the rmsd (Table 3).

3.5. Solvent Accessible Surface Area (SASA). Table 5 shows the percentage change of SASA for monomeric insulin chain-B systems under static electric field stress, relative to the NM300 system. The values are averaged over the data collection stage after the first 1 ns.

The SASA of the thermally stressed system was shown to decrease by 6% compared to the NM300 system, and qualitatively agrees with the r_g, where a decrease in overall size was observed. The SASA also stayed relatively constant for systems SM3 to SM5. The static field systems at the two highest field strengths showed much larger SASA compared to the reference systems, as a consequence of the stronger dipole moment coupling with the electric field due to the presence of chain-A. As discussed previously, the stronger coupling led to the stretching of the helical region, which caused the overall surface area to increase.

The variance of the SASA for the static field systems was shown to be of the same order as the NM300 system. There is a tendency for the variance to decrease as the electric field strength is increased again, indicating the restraining effect of the helical dipole moment.

In contrast to the results of the equivalent static field systems, the systems under oscillating field stress showed a decrease of overall SASA when the field strength was 10^8 V/m or lower. The average value of SASA for each of these systems is similar to the value obtained for the thermally stressed system (NM400). This indicates that the application of increased temperature or oscillating electric field of moderate strength causes insulin chain-B in a monomeric environment to adopt a more compact conformation. This suggests similarities in the mechanism of damage caused by both types of stress, where the mobility and flexibility of the protein are increased.

System OM1 showed a large change in SASA, which can be expected due to the high strength of the applied electric field. Systems OM2 and OM2H, however, had similar values of SASA, compared to the NM300 system. These systems are in contrast to their equivalent system under application of static electric field, which showed a much larger increase in SASA. This is due to the constant realignment of the protein with respect to the electric field which limits the stretching caused by the applied field. System OM2D showed smaller SASA with large variance, indicating that the protein has a similar conformation to the NM400 system, albeit with higher mobility and flexibility. The behavior of the oscillating field systems at 5×10^8 V/m is different from the behavior of the isolated insulin chain-B which showed a large increase in SASA, indicating more stretching damage in the isolated case. This is in agreement with the previous observation of the secondary structure (Figures 2 and 3).

The variance of the systems under oscillating electric field stress increases as the field strength is increased. This is in contrast to the behavior of the monomeric insulin under static electric field stress, which shows a decrease in variance. The increasing variance is a direct consequence of the oscillating nature of the electric field, which causes the protein to constantly align itself with respect to the applied field.

4. Conclusion

In this work, we have explored the behavior of the insulin hormone under ambient conditions and under applied stress conditions. A variety of structural and conformational analysis methods were employed to gain insight into the response of insulin chain-B to thermal stress and electric field in both static and oscillating forms within a range of frequencies and strengths.

Compared to the isolated form, insulin chain-B under monomeric conditions was observed to be very stable, owing to the presence of the disulfide bonds which tether it to chain-A. The presence of the disulfide bonds is important in preserving the secondary structure of the insulin monomer and was shown to inhibit the helix-breaking process of insulin chain-B (within the simulation time frame). These bonds enabled the molecule to withstand elevated temperature and electric field of strengths up to 10^8 V/m with minimal disruption to the secondary structure. The application of thermal stress was observed to increase the conformational mobility of the termini regions, although to a much lesser extent than in the isolated chain-B. Throughout the simulations, the B9−B19 α-helical core was maintained.

The presence of chain-A also affects the behavior of chain-B by contributing to the total helical dipole moment of the molecule. Under the application of static electric field stress, all three helical dipole moments—one arising from the helical region in chain-B and the other two from the helical regions in chain-A—interact with the applied field. This enables a lower field strength to cause disruption (stretching) to the secondary structure, compared to the isolated chain-B. In the monomeric insulin, this field strength was 5×10^8 V/m, whereas, in the isolated chain-B, it was 10^9 V/m.

Under the application of oscillating electric field, the presence of more than one helical region in a protein was also observed to interfere with the cooperative effect of the dipole moments. This is because the three helical regions simultaneously attempt

to align themselves with respect to the field, resulting in an increase of overall lag time for the whole protein to realign. In this case, there was relatively less damage to the protein structure compared to the equivalent system under the static electric field stress, the effect being more pronounced as the field strength is increased. At a field strength of 5×10^8 V/m, a frequency dependence was observed, with complete loss of secondary structure at field frequencies of 1.225 and 2.45 GHz but no observable structural change at a field frequency of 4.9 GHz. This is due to the rapid oscillation of the high frequency electric field, exposing the protein to short periods of "instantaneous" high strength electric field. Between the exposure periods, the protein experiences relaxation sufficient to repair the changes in secondary structure.

Acknowledgment. The authors wish to thank Dr Andrew Hung for helpful discussion. We acknowledge the Australian Research Council and Cytopia Pty. Ltd. for providing the funding for this project and the Australian Partnership for Advanced Computing for the grant of computation time.

References and Notes

(1) de Pomerai, D. I.; Smith, B.; Dawe, A.; North, K.; Smith, T.; Archer, D. B.; Duce, I. R.; Jones, D.; Candido, E. P. *FEBS Lett.* **2003**, *543*, 93.
(2) Salford, L. G.; Brun, A. E.; Eberhardt, J. L.; Malmgren, L.; Persson, B. R. R. *Environ. Health Perspect.* **2003**, *111*, 881.
(3) Laurence, J. A.; French, P. W.; Lindner, R. A.; McKenzie, D. R. *J. Theor. Biol.* **2000**, *206*, 291.
(4) Legge, F. S.; Budi, A.; Treutlein, H.; Yarovsky, I. *Biophys. Chem.* **2006**, *119*, 146.
(5) Budi, A.; Legge, S.; Treutlein, H.; Yarovsky, I. *Eur. Biophys. J.* **2004**, *33*, 121.
(6) Budi, A.; Legge, F. S.; Treutlein, H.; Yarovsky, I. *J. Phys. Chem. B* **2005**, *109*, 22641.
(7) Budi, A.; Legge, F. S.; Treutlein, H.; Yarovsky, I. *J. Phys. Chem. B* **2007**, *111*, 5748.
(8) Derewenda, U.; Derewenda, Z. S.; Dodson, G. G.; Hubbard, R. E. *Insulin Structure. In Insulin*; Cuatrecasas, P., Jacobs, S., Eds.; Springer-Verlag: Berlin, 1990; Vol. 92, p 23.
(9) Liang, D.-C.; Chang, W.-R.; Zhang, J.-P.; Wan, Z.-L. *Sci. China, Ser. B* **1992**, *35*, 547.
(10) Bentley, G.; Dodson, E.; Dodson, G.; Hodgkin, D.; Mercola, D. *Nature* **1976**, *261*, 166.
(11) Derewenda, U.; Derewenda, Z.; Dodson, E. J.; Dodson, G. G.; Reynolds, C. D.; Smith, G. D.; Sparks, C.; Swenson, D. *Nature* **1989**, *338*, 594.
(12) Whittingham, J. L.; Chaudhuri, S.; Dodson, E. J.; Moody, P. C. E.; Dodson, G. G. *Biochemistry* **1995**, *34*, 15553.
(13) Blundell, T.; Dodson, G.; Hodgkin, D.; Mercola, D. *Adv. Protein Chem.* **1972**, *26*, 279.
(14) Jørgensen, A. M. M.; Olsen, H. B.; Balschmidt, P.; Led, J. J. *J. Mol. Biol.* **1996**, *257*, 684.
(15) Olsen, H. B.; Ludvigsen, S.; Kaarsholm, N. C. *Biochemistry* **1996**, *35*, 8836.
(16) Hua, Q. X.; Shoelson, S. E.; Inouye, K.; Weiss, M. A. *Proc. Natl. Acad. Sci. U.S.A.* **1993**, *90*, 582.
(17) Dong, J.; Wan, Z. L.; Popov, M.; Carey, P. R.; Weiss, M. A. *J. Mol. Biol.* **2003**, *330*, 431.
(18) Hua, Q. X.; Weiss, M. A. *Biochemistry* **1991**, *30*, 5505.
(19) Hua, Q.-X.; Hu, S.-Q.; Frank, B. H.; Jia, W. H.; Chu, Y.-C.; Wang, S.-H.; Burke, G. T.; Katsoyannis, P. G.; Weiss, M. A. *J. Mol. Biol.* **1996**, *264*, 390.
(20) Pittman, I., IV.; Tager, H. S. *Biochemistry* **1995**, *34*, 10578.
(21) Zoete, V.; Meuwly, M.; Karplus, M. *J. Mol. Biol.* **2004**, *342*, 913.
(22) Zhang, Y.; Whittingham, J. L.; Turkenburg, J. P.; Dodson, E. J.; Brange, J.; Dodson, G. G. *Acta Crystallogr., Sect. D* **2002**, *58*, 186.
(23) Ludvigsen, S.; Olsen, H. B.; Kaarsholm, N. C. *J. Mol. Biol.* **1998**, *279*, 1.
(24) Dodson, E. J.; Dodson, G. G.; Hubbard, R. E.; Reynolds, C. D. *Biopolymers* **1983**, *22*, 281.
(25) Derewenda, U.; Derewenda, Z.; Dodson, E. J.; Dodson, G. G.; Bing, X.; Markussen, J. *J. Mol. Biol.* **1991**, *220*, 425.
(26) Hawkins, B.; Cross, K.; Craik, D. *Int. J. Pept. Protein Res.* **1995**, *46*, 424.
(27) Qiao, Z.-S.; Min, C.-Y.; Hua, Q.-X.; Weiss, M. A.; Feng, Y.-M. *J. Biol. Chem.* **2003**, *278*, 17800.
(28) Badger, J.; Harris, M. R.; Reynolds, C. D.; Evans, A. C.; Dodson, E. J.; Dodson, G. G.; North, A. C. T. *Acta Crystallogr., Sect. B* **1991**, *47*, 127.
(29) Ciszak, E.; Beals, J. M.; Frank, B. H.; Baker, J. C.; Carter, N. D.; Smith, G. D. *Structure* **1995**, *3*, 615.
(30) Yao, Z.-P.; Zeng, Z.-H.; Li, H.-M.; Zhang, Y.; Feng, Y.-M.; Wang, D.-C. *Acta Crystallogr., Sect. D* **1999**, *55*, 1524.
(31) Kaarsholm, N. C.; Ko, H.-C.; Dunn, M. F. *Biochemistry* **1989**, *28*, 4427.
(32) Allen, M. P.; Tildesley, D. J. *Computer Simulation of Liquids*; Oxford University Press: New York, 1989.
(33) Leach, A. R. *Molecular Modelling: Principles and Applications*, 2nd ed.; Prentice Hall: Harlow, England, 2001.
(34) Kalé, L.; Skeel, R.; Bhandarkar, M.; Brunner, R.; Gursoy, A.; Krawetz, N.; Phillips, J.; Shinozaki, A.; Varadarajan, K.; Schulten, K. *J. Comput. Phys.* **1999**, *151*, 283.
(35) MacKerell, A. D., Jr.; Bashford, D.; Bellott, M.; Dunbrack, R. L., Jr.; Evanseck, J. D.; Field, M. J.; Fischer, S.; Gao, J.; Guo, H.; Ha, S.; Joseph-McCarthy, D.; Kuchnir, L.; Kuczera, K.; Lau, F. T. K.; Mattos, C.; Michnick, S.; Ngo, T.; Nguyen, D. T.; Prodhom, B.; Reiher, W. E., III; Roux, B.; Schlenkrich, M.; Smith, J. C.; Stote, R.; Straub, J.; Watanabe, M.; Wiórkiewicz-Kuczera, J.; Yin, D.; Karplus, M. *J. Phys. Chem. B* **1998**, *102*, 3586.
(36) Darden, T.; York, D.; Pedersen, L. *J. Chem. Phys.* **1993**, *98*, 10089.
(37) Essmann, U.; Perera, L.; Berkowitz, M. L.; Darden, T.; Lee, H.; Pedersen, L. G. *J. Chem. Phys.* **1995**, *103*, 8577.
(38) Petersen, H. G. *J. Chem. Phys.* **1995**, *103*, 3668.
(39) Ryckaert, J.-P.; Ciccotti, G.; Berendsen, H. J. C. *J. Comput. Phys.* **1977**, *23*, 327.
(40) Berman, H. M.; Westbrook, J.; Feng, Z.; Gilliland, G.; Bhat, T. N.; Weissig, H.; Shindyalov, I. N.; Bourne, P. E. *Nucleic Acids Res.* **2000**, *28*, 235.
(41) Jorgensen, W. L.; Chandrasekhar, J.; Madura, J. D.; Impey, R. W.; Klein, M. L. *J. Chem. Phys.* **1983**, *79*, 926.
(42) Feller, S. E.; Zhang, Y. H.; Pastor, R. W.; Brooks, B. R. *J. Chem. Phys.* **1995**, *103*, 4613.
(43) Frishman, D.; Argos, P. *Proteins: Struct., Funct., Genet.* **1995**, *23*, 566.

JP800350V